

# Improved Integrated Waveguide Absorbance Optodes for Ion-Selective Sensing

Mar Puyol,<sup>†</sup> Íñigo Salinas,<sup>‡</sup> Ignacio Garcés,<sup>‡</sup> Francisco Villuendas,<sup>‡</sup> Andreu Llobera,<sup>§</sup> Carlos Domínguez,<sup>§</sup> and Julián Alonso<sup>\*,†</sup>

*Sensors & Biosensors Group, Department of Chemistry, Autonomous University of Barcelona, Edifici Cn, 08193 Bellaterra, Catalonia, Spain, Dpto. Física Aplicada, Universidad de Zaragoza, Spain, and Centro Nacional de Microelectrónica, 08193 Bellaterra, Catalonia, Spain*

**The first prototype of a technologically improved integrated waveguide absorbance optode (IWAO) was developed and tested with a membrane based on a new H<sup>+</sup>-selective ketocyanine dye and a cadmium ionophore. It was designed with curved instead of rectilinear planar waveguides. Results demonstrated the suitability of the new IWAOs to be employed as sensing platforms, which confer versatility, robustness, and mass production capabilities besides high sensitivity on conventional bulk optodes, as well as the usefulness of such dyes in developing ion-selective membranes in combination with a selective ionophore. The sensor integration as a detector in a flow injection system (FIA) was proposed to obtain an automated, simple, and sufficiently reproducible (RSD <5%) analytical methodology with a sample throughput of 55 h<sup>-1</sup>. Very sensitive optodes were obtained, and detection limits on the order of 20 ppb were achieved. Because of the ionophore employed, the optode system showed excellent selectivity over alkali and alkaline-earth metals with the exception of samples containing lead and cadmium ions, where the membrane responded to both analytes. The proposed procedure combines all the advantages of the FIA systems, the simplicity of optical detection, ion recognition selectivity, and sensitivity of ketocyanine dyes, and the features achieved using the integrated device, which comprise an improved sensitivity and short response times as well as robustness, easy handling, and mass production.**

Trends in the optical sensor field are the combination of traditional bulk optodes with fiber optics to exploit the technological improvements attained by the telecommunication industry. An even more promising technology is planar waveguide chemical sensing<sup>1-4</sup> as it allows the implementation of automated mass fabrication methodologies. The advantages that the concept of an

integrated waveguide absorbance optode (IWAO) can provide in the field of optical sensors based on ion-selective polymeric membranes were previously reported.<sup>5,6</sup> We present some important technological modifications that have been performed to obtain a rugged sensor, which permit a practical coupling between optical fibers and waveguides by separating the optical and communication systems from the optochemical transducer. It mainly consists of a microfabricated circuit of curved Arrow planar waveguides and a chemically active membrane. The membrane is deposited over the circuit and covers a well-defined area between the planar waveguides. Because of its composition, thickness (4 μm), and refractive index ( $n = 1.46$ ), it acts as the recognition element and as a part of the guiding structure of the sensor. The optode is based on absorbance measurements. The optochemical transduction mechanism is established when light coming from the source is guided through an input curved planar waveguide to the ion recognition membrane, which changes its spectroscopic properties while it interacts with the analyte from the sample solution and guides the modulated light to an output rectilinear planar waveguide.

Recently, some ketocyanine dyes have been characterized in devices based on rectilinear planar waveguides, demonstrating their capability to be employed as chromoionophores in polymeric membranes to develop pH-sensitive integrated waveguide optical sensors,<sup>7</sup> but their suitability to develop highly sensitive ion-selective integrated optical sensors has not been already proved.

The aim of the present work is to present a versatile platform for optical sensing, which offers improved response characteristics on conventional bulk optodes as higher sensitivity with low response times, due to its unique configuration and the use of very sensitive ketocyanine dyes, and improved technological characteristics such as portability, easy activation or removal of the membrane, low-cost construction, and the possibility to perform continuous monitoring as in situ measurements. The paper presents the development of an ion-selective optode, combining one ketocyanine dye with a selective ionophore, and its incorporation in a technologically improved integrated device

\* Corresponding author: (e-mail) jach@gsb.uab.es.

<sup>†</sup> Autonomous University of Barcelona.

<sup>‡</sup> Universidad de Zaragoza.

<sup>§</sup> Centro Nacional de Microelectrónica.

(1) Dessy, R. E. *Anal. Chem.* **1989**, *61*, 233–240.

(2) Tóth, K.; Zagy, G.; Lau, B. T. T.; Jeney, J.; Choquette, S. J. *Anal. Chim. Acta* **1997**, *353*, 1–10.

(3) Benaisa, K.; Nathan, A. *Sens. Actuators, A* **1998**, *65*, 33–44.

(4) Brecht, A.; Gauglitz, G. *Sens. Actuators, B* **1997**, *38–39*, 1–7.

(5) Puyol, M.; del Valle, M.; Garcés, I.; Villuendas, F.; Domínguez, C.; Alonso, J. *Anal. Chem.* **1999**, *71*, 5037–5044.

(6) Garcés, I.; Villuendas, F.; Subías, J.; Alonso, J.; del Valle, M.; Domínguez, C. *Opt. Lett.* **1997**, *23*, 225–227.

(7) Puyol, M.; Miltsov, S.; Salinas, I.; Alonso, J. *Anal. Chem.* **2002**, *74*, 570–576.

to obtain a highly sensitive and portable optical system for an in situ chemical analysis.

The toxic effects of heavy metals in the environment have been demonstrated by a great number of studies<sup>8–11</sup> and their uncontrolled introduction into the environment has caused serious concern. Among all the toxic heavy metals, cadmium compounds are very harmful at low concentrations, making necessary their determination in environmental samples. Because of the extensive use of cadmium in industrial processes, it can reach a high concentration in areas immediately adjacent to mines, smelters, and Ni–Cd battery plants. Actually, the problem is not restricted only to these focused points but also to a diffuse contamination. Cadmium is deposited in a much more widespread distribution as a result of the agricultural practice of using contaminated phosphate fertilizers<sup>12</sup> such as treated urban sewage sludge, and therefore, its concentration is increasing in both aquatic and terrestrial environments. In many countries, new legislation has been developed to reduce the load of cadmium on the environment. The European Commission has set the limit of the maximum admissible concentration of cadmium (MAC) in sludge for agricultural application to 3 ppm.<sup>13</sup> Therefore, it would be essential to obtain a highly sensitive and selective procedure for in situ cadmium determination, which conforms to the tolerated levels defined by the law.

Actually, the methods generally used in analytical control laboratories are atomic absorption spectrophotometry and inductively coupled plasma mass spectrometry. They permit selective detection of cadmium over other metals with very low detection limits (1 ppb), but with the difficulty of a complex infrastructure and high-cost equipment that prevents its application for in situ measurements in real time. Numerous spectrophotometric<sup>14–16</sup> and electrochemical methods have been developed for this purpose. Among the last ones, the commercially available crystalline membrane electrodes (CdS/Ag<sub>2</sub>S electrodes)<sup>17–19</sup> are noteworthy. They reach low detection limits (10 ppb), but they suffer significant interference from other heavy metals such as Ag<sup>+</sup>, Cu<sup>2+</sup>, Hg<sup>2+</sup>, Fe<sup>3+</sup>, and Pb<sup>2+</sup>. Much of the research work has been invested in the study of selective ionophores, basically electrically neutral carriers, to develop cadmium-selective sensors with low detection limits. Although, initially, they have been characterized in ISE membranes,<sup>20–26</sup> there is an increasing interest in using them in

bulk optodes<sup>27</sup> because of the enhanced sensitivity offered by optical transduction methods. In this way, we have developed a cadmium-selective membrane combining one of the previously characterized ketocyanine dyes<sup>7</sup> with a commercially available oxamide. The absorbance maximum of the ketocyanine dye matches the wavelength of the employed diode laser (780 nm) and provides a high capacity to differentiate between small concentration variations as a result of its high molar absorptivity. The employed ionophore was previously reported as a lead ionophore,<sup>28,29</sup> but in this work, it assigns cadmium selectivity to the membrane as well.

A continuous-flow approach is often used to characterize bulk optodes, but only a few applied flow injection systems have been reported to date<sup>30–34</sup> due to the long response times of the conventional bulk optodes needed to guarantee good sensitivity. The present paper proposes a FIA system for the determination of cadmium in water using an improved integrated cadmium-selective waveguide absorbance optode, because the configuration of the IWAOs permits enhanced sensitive signals in short response times, taking advantage of the very thin membranes deposited over the circuit.

## EXPERIMENTAL SECTION

**Apparatus.** Spectra of the PVC bulk optode were done between 830 and 400 nm using a double-beam UV–visible–NIR scanning spectrophotometer (Shimadzu UV-310PC).

The FIA system used for the determination of cadmium in water is depicted in Figure 1. It consisted of a Gilson Minipuls 3 peristaltic pump, equipped with PVC pump tubing (Elkay, Boston, MA), a six-way valve (Hamilton MVP) as the injection system with a suitable length of sampling loop, and a laboratory-made tee connection with a short input tubing to ensure the renewal of the sample. Flow lines were built using PTFE 0.8-mm-i.d. tubing. An improved IWAO prototype based on curved waveguides of a 500- $\mu$ m-long cavity for the recognition region was used. A flow cell similar to a wall-jet layout was used to evaluate its response. The optical source was a diode laser (GCA Fiberoptics, GCA-78MI) emitting at 778 nm with 33-nm spectral width. Working under the threshold current (nonlasing action), it couples 11.26  $\mu$ W of optical power to the device. Fiber-emitter and fiber-detector coupling was accomplished using standard optical fiber connectors. The detector was a Pin photodiode connected to a transimpedance preamplifier. The signal was amplified and filtered using a lock-in

- (8) Casarett, D. *Toxicology: The Basic Science of Poisons*, 5th ed.; MacGraw-Hill: New York, 1996.
- (9) Katzung, B. G. *Basic and Clinical Pharmacology*, 3rd ed.; Appleton and Lange: Norwalk, CT, 1987.
- (10) Ward, N. *Trace Elem. Man Anim.* **1993**, *8*, 872.
- (11) Friberg, L.; Elinder, C. G.; Kjellström, T. *Cadmium*; World Health Organization: Geneva, 1992.
- (12) The Fertilizer Industry of the European Industry. *Agriculture, Fertilizers and the Environment*; EFMA: Brussels, 1997.
- (13) Directive 86/278/EEC. [http://europa.eu.int/comm/environment/sludge/sludge\\_disposal2.pdf](http://europa.eu.int/comm/environment/sludge/sludge_disposal2.pdf)
- (14) Ertaş, N.; Akkaya, E. U.; Ataman, O. Y. *Talanta* **2000**, *51*, 693–699.
- (15) Taverna, P. J.; Mayfield, H.; Andrews, A. R. *J. Anal. Chim. Acta* **1998**, *373*, 111–117.
- (16) Yamane, T.; Yamaguchi, Y. *Anal. Chim. Acta* **1997**, *345*, 139–146.
- (17) *Handbook of Ion-Selective Electrodes. Selectivity Coefficients*; CRC Press: Boca Raton, FL, 1990.
- (18) Ferreira, I. M. P. L. V. O.; Lima, J. L. F. C. *Analyst* **1994**, *119*, 209–212.
- (19) Couto, C. M. C. M.; Lima, J. L. F. C.; Montenegro, C. B. S. M.; Reis, B. F.; Zaggato, E. A. G. *Anal. Chim. Acta* **1998**, *366*, 155–161.
- (20) Gupta, V. K.; Kumar, P. *Anal. Chim. Acta* **1999**, *389*, 205–212.
- (21) Ion, A. C.; Bakker, E.; Pretsch, E. *Anal. Chim. Acta* **2001**, *440*, 71–79.

- (22) Piñeros, M. A.; Shaff, J. E.; Kochian, L. V.; Bakker, E. *Electroanalysis* **1998**, *10*, 937–941.
- (23) Javanbakht, M.; Shabani-Kia, A.; Darvich, M. R.; Ganjali, M. R.; Shamsipur, M. *Anal. Chim. Acta* **2000**, *408*, 75–81.
- (24) Stevens, A. C.; Freiser, H. *Anal. Chim. Acta* **1991**, *248*, 315.
- (25) Srivastava, S. K.; Gupta, V. K.; Jain, S. *Electroanalysis* **1996**, *8*, 938.
- (26) Cobben, P. L. H. M.; Egberink, R. J. M.; Bomer, J. B.; Bergveld, P.; Verboom, W.; Reinhoudt, D. N. *J. Am. Chem. Soc.* **1992**, *114*, 1029.
- (27) Bühlmann, P.; Pretsch, E.; Bakker, E. *Chem. Rev.* **1998**, *98*, 1593–1687.
- (28) Lerchi, M.; Bakker, E.; Rusterholz, B.; Simon, W. *Anal. Chem.* **1992**, *64*, 1534–1540.
- (29) Bakker, E.; Willer, M.; Pretsch, E. *Anal. Chim. Acta* **1993**, *282*, 265–271.
- (30) Wolfbeis, O. S. *J. Mol. Struct.* **1993**, *292*, 133.
- (31) Hisamoto, H.; Nakagawa, E.; Nagatsuka, K.; Abe, Y.; Sato, S.; Siswanta, D.; Suzuki, K. *Anal. Chem.* **1995**, *67*, 1315.
- (32) Hauser, P. C.; Litten, J. C. *Anal. Chim. Acta* **1994**, *294*, 49.
- (33) Hisamoto, H.; Satoh, S.; Satoh, K.; Tsubuku, M.; Siswanta, D.; Shichi, Y.; Koike, Y.; Suzuki, K. *Anal. Chim. Acta* **1999**, *396*, 131–141.
- (34) Sotomayor, P. T.; Raimundo, I. M., Jr.; Neto, G. de O.; de Oliveira, W. A. *Sens. Actuators, B* **1998**, *51*, 382–390.

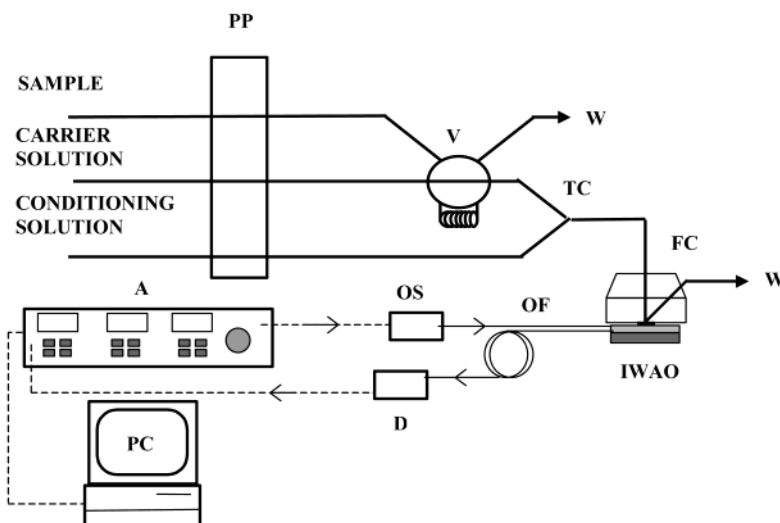


Figure 1. FIA system used for the determination of cadmium in water samples. PP, peristaltic pump; V, six-way injection valve with a determined injection volume; W, waste; TC, tee connector; FC, flow cell; IWAO, integrated waveguide absorbance optode incorporating the cadmium-selective bulk optode; OF, optical fibers; OS, optical source consisting of a diode laser (778 nm); A, lock-in amplifier; D, Pin photodiode; PC, personal computer; (—) flow lines; (---) communication lines.

amplifier (SR810 DSP Stanford Research Systems) that also tuned the modulation frequency of the laser source (1.1 kHz). The analytical signal was collected and treated by a PC. The necessary software to control the data acquisition was written in Visual Basic 5.0.

**Reagents.** All of the chemicals were of analytical reagent grade. Metal solutions were prepared by dilution of a  $1 \times 10^{-2}$  M stock solution, which was prepared by direct weighing of the corresponding nitrate salt (Merck, Darmstadt, Germany) and dilution in doubly distilled water. The FIA conditioning solution was a 0.1 M acetic/acetate buffer adjusted to a selected pH using concentrated acetic acid. The carrier solution was double-distilled water. For membrane preparation, the following components were obtained from Fluka (Buchs, Switzerland): poly(vinyl chloride) (PVC high molecular weight) as the polymer, bis(2-ethylhexyl) sebacate (DOS) as the plasticizer, and tetrahydrofuran (THF) as the solvent; potassium tetrakis(4-chlorophenyl)borate (KTPCIPB) was used as the lipophilic anionic additive; and *N,N,N,N*-tetradodecyl-3,6-dioxaoctanedithioamide (ETH 5435) was used as the cadmium ionophore. The ketocyanine 5ee used as the chromoionophore was synthesized in our laboratory.<sup>35</sup>

**Membrane Preparation.** Membrane components were weighed out and dissolved in 1.5 mL of THF to prepare the cocktail solution. The composition consisted of 0.3 wt % ketocyanine 5ee, 0.3 wt % KTPCIPB, 12.8 wt % ETH 5435, 28.1 wt % PVC, and 58.5 wt % DOS. To obtain membranes of a thickness matching the height of the waveguide core (4- $\mu$ m, measured using confocal microscopy<sup>36,37</sup>) and then achieve light guidance, the following deposition technique was employed. A 50- $\mu$ L aliquot of a diluted cocktail (1:2) in THF was dropped onto the device and quickly expanded over the silicon surface of the IWAO, with the aid of a microscope slide (reproducing the screen-printing deposi-

tion technique), allowing THF evaporation. Results demonstrated that the reproduced deposition procedure gave a thickness near the optimum. Moreover, an indirect evaluation method, which consisted of the light loss measurement, corroborated it, as the obtained light losses were equivalent to the ones acquired with 4- $\mu$ m-thickness membranes (5–10 dB).

## RESULTS AND DISCUSSION

To demonstrate the possibilities that the use of an IWAO offers in the field of optical sensing, the aim of the present work was the development of a cadmium-selective optical sensor prototype, which fulfilled features such as high sensitivity, easy handling, and easy assembly. In addition, we wanted to provide an economical, rugged, easily automated, and portable measurement system of a high sample throughput for future routine analysis. Hence, we selected the flow injection technique to satisfy these requirements.

Since ion-selective optodes based on ion exchange mediated by an ionophore and an indicator sense the ratio of the analyte and hydrogen ions in the sample solution, the pH had to be kept constant. As is well known, the FIA technique is based on the injection of a certain sample volume in a carrier solution, which is continuously directed to the detector. It easily allows adding a conditioning channel that buffers the inserted sample before the detection, even though a sample dilution occurs. Figure 1 shows the simple FIA manifold used. Since the blank signal was taken at the baseline generated by the buffer solution half diluted (fully protonated chromoionophore) an absorbance decrease was recorded when cadmium samples reached the optode.

As is mentioned in the introduction, with the intention of improving robustness and simplifying sensor integration as a detector in flow systems or sensor employment for in situ measurements, we wanted to construct a new exchangeable transducer, which could be easily and reversibly coupled to optical fibers in a way that waveguide activation (deposition of the membrane) could be performed using reproducible deposition techniques (such as the spin-coat technique) or that the sensor

(35) Miltsov, S.; Encinas, C.; Alonso, J. *Tetrahedron Lett.* **2001**, *42*, 6129–6131.

(36) Laguarda, F.; Artigas, R.; Pintó, A.; Al-Khatib, I. *Proc. SPIE-Int. Soc. Opt. Eng.* **1998**, *3520*, 149–160.

(37) Artigas, R.; Pintó, A.; Laguarda, F. *Proc. SPIE-Int. Soc. Opt. Eng.* **1999**, *3824*, 93–104.

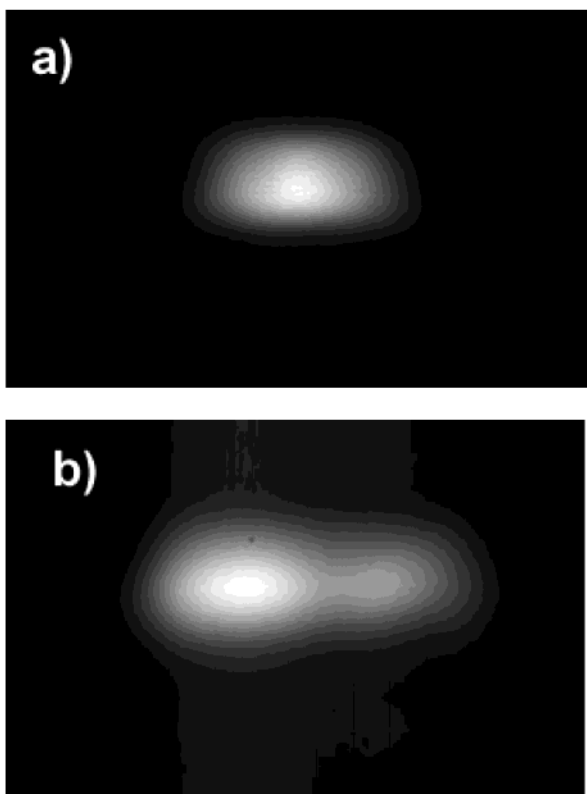


Figure 2. Optical power at the exit of two Arrow structures of (a) 8- and (b) 20- $\mu\text{m}$  width.

could be regenerated using disposable transducers when the response characteristics of the membrane were quenched. For this reason, both input and output waveguides had to be constructed at the same side of the device, and hence, one had to reverse direction. The fabrication process of the new transducer is based on the same complementary metal oxide semiconductor (CMOS) compatible processes over a silicon wafer, employed for the construction of the previous integrated rectilinear planar Arrow sensors,<sup>38–41</sup> but some changes related to the masks, which define the curves and the connection platform, were done.

**Optical Characterization.** The developed sensor is based on input and output rib Arrow waveguides of 20- and 50- $\mu\text{m}$  widths, respectively. The characteristics of the Arrow structure make it so that there is only a single-mode profile in the direction transverse to the layers and possibly a multimode profile in the direction lateral to the layers, depending on the waveguide width. To thoroughly explain this concept, it is useful to look at the far-field images of Figure 2 captured by CCD camera at the exit of two Arrow waveguides of different widths.

Figure 2a shows one light propagation pattern in the transverse direction (vertical axis) as well as in the lateral direction

(horizontal axis) to the layers. As this pattern is unaltered when the waveguide excitation conditions are changed, it leads one to conclude that the waveguide profile is single mode. Figure 2b shows one light propagation pattern in the direction transverse to the layers due to the antiresonant effect of the Arrow waveguide, while in the lateral direction, a more complex guiding structure can be observed due to the existing different guiding modes. Again, this effect is confirmed when the excitation conditions of the waveguide are changed, as a change in the modal pattern can be observed in the direction lateral to the layers. Therefore, it is possible to assert that the modal light distribution of the employed Arrow structures is single mode in the direction transverse to the layers while is multimode in the direction lateral to the layers. Using multimode waveguides does not involve instabilities due to uncontrolled variations in the modal structure, because only the guiding conditions and the excitation conditions can affect the modal distribution. They will not be modified owing to the waveguide isolation from the external medium by an upper layer (1.46) and the stick of optical fibers and waveguides. The reason such wider Arrow waveguides were employed is the requirement of simplifying sensor construction, as narrow waveguides present critical tolerances in the alignment of the optical fibers to the Arrow waveguides.

As is mentioned in the introduction, an open region between the input and the output waveguides, where the optical membrane is deposited, defines the recognition region. As the antiresonant structure is still present under the membrane and its thickness is designed to be the same as the height of the waveguide core, a single-mode light distribution is expected in the membrane in the direction transverse to the layers but it acts as a free propagation region in the direction lateral to the layers. As the membrane is not strictly a waveguide, but a free region where light remains guided performing an Arrow distribution in the transverse direction, it is difficult to state the mode profile.

The membrane refractive index is near 1.46, but small refractive index variations will not affect the guided field distribution in the membrane, as it does not show a particular lateral distribution in the transverse direction. Membrane propagation losses are due to light losses in the input waveguide–membrane light coupling, light diffraction in the direction lateral to the layers, which is not coupled to the output waveguide because the rib structure is eliminated, and light losses in the membrane–output waveguide light coupling. They have been measured to be  $\sim 6$  dB for a 500- $\mu\text{m}$  optical path length.

Additional light losses occur with the new curved pattern. Light losses due to the curvature of the Arrow waveguides were studied for different curvature radii. Figure 3a shows light attenuation due to the waveguide curvature for 20- and 50- $\mu\text{m}$ -width curved and rectilinear waveguides. As should be expected, the higher the radius the lower the light losses due to the electromagnetic field effect in the curved region. Although the obtained light losses are less than 2 dB/cm (including light losses of the Arrow themselves) for 3 mm or higher radii, it is interesting to determine the total light attenuation of the device, because longer waveguides of higher intrinsic light losses have to be constructed for higher waveguide curvature radii of 180° turns. The experimental data are shown in Figure 3b, where light losses are depicted for 20- $\mu\text{m}$ -width curved waveguides.

(38) Moreno, M.; Domínguez, C.; Muñoz, F.; Calderer, J.; Morante, J. R. *Sens. Actuators, A* **1997**, *62*, 524–528.

(39) Moreno, M.; Garcés, I.; Muñoz, J.; Domínguez, C.; Calderer, J.; Villuendas, F.; Pelayo, J. *Advances in science and technology: advanced materials in optics, electro-optics and communication technologies*; P. Vinzencini: Faenza, 1995; Vol. 11, pp 465–472.

(40) Moreno, M.; Muñoz, J.; Garrido, B.; Samitier, J.; Calderer, J.; Domínguez, C. *Advances in science and technology: advances in inorganic films and coatings*; P. Vinzencini: Faenza, 1995; Vol. 5, pp 149–154.

(41) Domínguez, C.; Muñoz, J.; González, R.; Tudanca, M. *Sens. Actuators, A* **1993**, *37–38*, 779–783.

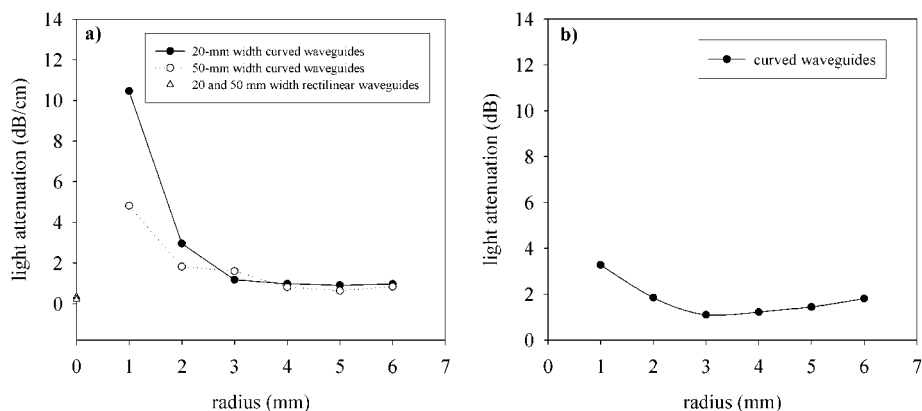


Figure 3. Light attenuation for different curvature radii of 20- and 50- $\mu\text{m}$  width curved and rectilinear waveguides. (a) Light losses due to the curvature of the Arrow waveguides; (b) total light losses of the device due to the waveguide curvature and length.

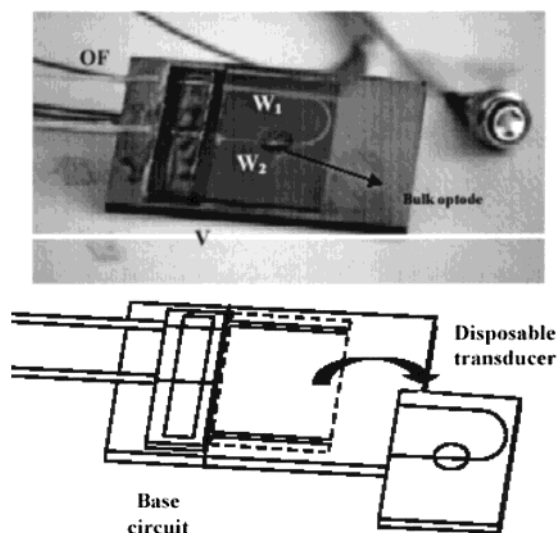


Figure 4. Photograph of one of the developed improved sensors based on curved planar waveguides. OF, optical fibers; W1, input waveguide; W2, output waveguide; V, V-grooves. The schematic picture simulates the coupling/decoupling of the exchangeable transducer to the base platform, which includes optical fibers, V-grooves, and rectilinear waveguides.

Although light attenuation does not rise above the 2 dB values for a 2–6-mm radius range, there is a light loss minimum for a 3-mm radius. Despite showing a slightly light attenuation increase of 1.32 dB in comparison with the minimum, a 6-mm-curvature radius waveguide was chosen taking into account the final transducer dimensions, which are subject to the required distance between the input and the output waveguides to allow the flow cell adaptation.

Figure 4 shows a photograph of one of the new sensors and a picture reproducing the future allowed coupling/decoupling of the transducer to the base circuit. For descriptive purposes, the polymeric membrane was deposited only in the cut area between waveguides and it can be distinguished in the picture after the curve. However, a screen-printing-like deposition technique was used for this work covering the entire circuit of the disposable transducer.

**Optimization of the Flow System.** To generate the bulk optode signal, a condition near the equilibrium between the bulk of the membrane and the sample must be reached, and response

time is often determined by the time to attain a uniform concentration of the components in the membrane. Hence, diffusion within the polymeric membrane is time limiting. Since the FIA technique produces a nonequilibrated transitory signal, hydrodynamic parameters must be carefully selected to allow signal reproducibility. Initially, the influence of flow rate and injection volume on sensitivity and response time was studied (Figure 5a). In these experiments, a 1 ppm cadmium solution was injected in triplicate in a 0.1 M acetic acetate buffer at pH 5.01. In accordance with optode kinetic responses in flow conditions, the analytical signal depends on the time interval in which the membrane is in contact with the sample, until the steady-state signal is reached, but ion diffusion on the membrane and effects such as dispersion of the sample into the carrier solution, or sample carry-over, must be taken into account.

As Figure 5 shows, each sample volume has an optimum flow rate, in which a maximum sensitivity is attained. We considered the analysis time as well. It is defined by the interval time from the sample insertion to the baseline signal return (5% of the peak height). As was expected, sample throughput increased with flow rate, if a minimum contact time between membrane and sample solution was guaranteed, but it decreased when sample volume or sample dispersion increased (small sample volumes and slow sample rates).

As a compromise between sampling rate and analytical sensitivity, an injection volume of 300  $\mu\text{L}$  and a flow rate of 2.1 mL/min were chosen. With this optimized system, a sampling throughput of 55  $\text{h}^{-1}$  was attained for a 0.01–1000 ppm Cd range.

**Sensitivity and Detection Limit.** The composition of the conditioning solution was studied to obtain the best detection limit, the highest sensitivity, and a convenient linear range. A 0.1 M acetic/acetate buffer was chosen knowing beforehand the influence of its concentration in the response time of a bulk optode. The dependence of the pH value of the conditioning sample on the optical signal can be exploited to tune the sensitivity range to the target sample concentration. Four different pH values, in the 4.5–6.0 pH range, were tested. Such a pH range guaranteed the buffering capability of the 0.1 M acetic/acetate solution and assured the presence of free cadmium ions in the mixed solution after the sample injection. We can see in Figure 6 that the measuring range of the calibration curves was shortened as pH increased.

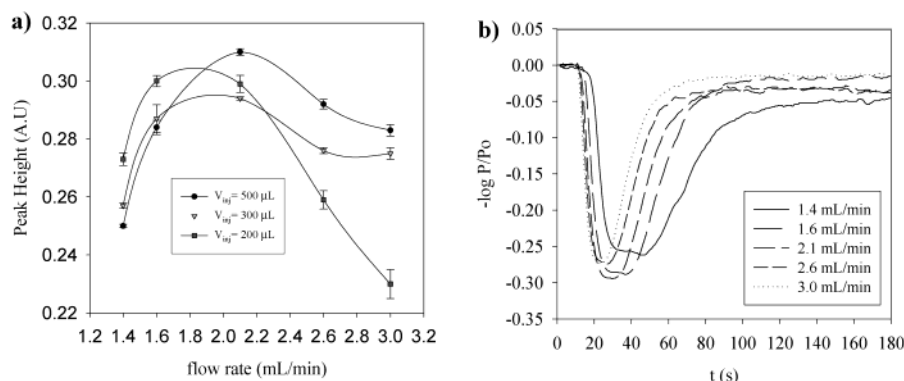


Figure 5. Effect of the hydrodynamic parameters in the FIA system for 1 ppm cadmium sample inserted in triplicate in a 0.1 M acetic/acetate buffer at pH 5.01. (a) For each sample volume, different flow rates (mL/min) were used; 1.4, 1.6, 2.1, 2.6, and 3.0 and the obtained signal reproducibility conforms to RSD = 0.2–4.5%, depending on the FIA conditions. (b) One of the FIA peak triplicates recorded for a sample volume of 300  $\mu\text{L}$  at different flow rates. A high dispersion of the sample can be observed at slow sample rates and, consequently, a delay in the baseline return.

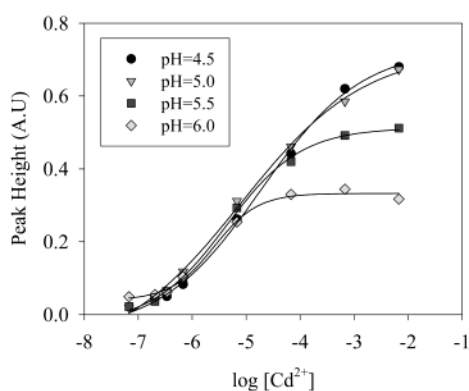


Figure 6. Calibration curves obtained with the cadmium-selective integrated waveguide sensor using 300- $\mu\text{L}$  sample volumes at a flow rate of 2.1 mL/min for various pH values of the 0.1 M acetic/acetate conditioning solution.

The obtained FIA peaks are relative to the baseline signal, determined by the pH of the conditioning system. For a higher pH value, a lesser amount of protonated chromoionophore is able to release its proton and allow the cationic exchange. The detection limit was determined graphically in analogy to other analytical methods, as the intersection of the theoretical response curve with the highest value of the error bar from the standard deviation of the signal without analyte ions. Table 1 summarizes the obtained results varying the pH of the conditioning solution. While the effect of pH over the upper detection limit was notable, the lower detection limit remained almost invariable from a certain pH. This may be due to the interference of the background electrolyte of the conditioning solution. However, it would be possible to improve the detection limit without compromising sensitivity by lowering the chromoionophore concentration, because besides ketocyanine dyes present very high molar absorptivities, the long path length of the integrated device ensures sensitivity.

Another excellent alternative for the optimization of the detection limit while maintaining high sensitivity would be changing the chromoionophore basicity, thus using one of the other reported well-behaved ketocyanine dyes.<sup>7</sup> For this particular membrane composition and with the prefixed flow conditions, pH 5 was selected as the optimum for the lowest detection limit (1.6

Table 1. Effect of Conditioning Sample pH on the Cadmium Determination

pH	linear range (M)	sensitivity (UA/decade)	detection limit <sup>a</sup> (M)
4.5	$4.7 \times 10^{-7}$ – $1.7 \times 10^{-3}$	0.179	$4.6 \times 10^{-7}$
5.0	$2.3 \times 10^{-7}$ – $4.0 \times 10^{-4}$	0.171	$1.6 \times 10^{-7}$
5.5	$2.4 \times 10^{-7}$ – $7.9 \times 10^{-5}$	0.173	$1.9 \times 10^{-7}$
6.0	$3.0 \times 10^{-7}$ – $1.9 \times 10^{-5}$	0.148	$2.7 \times 10^{-7}$

<sup>a</sup> Calculated from the standard deviation of the signal without analyte ions ( $6\Delta\alpha$ ).

$\times 10^{-7}$  M cadmium concentration) and a highly sensitive response (0.171 UA/decade) in a reasonable measuring range for environmental applications. In comparison to conventional transmission configurations, slopes of 0.063 UA/decade were obtained using the same membrane composition.

**Interferences.** Once the system was properly optimized, we proceeded to evaluate the cadmium selectivity of the membrane over a range of alkali, alkaline-earth, and heavy metals by performing a fixed interference method (FIM) since it reproduced the final situation of the analytical measurement more closely. Each cadmium calibration experiment was determined in solutions that contained a constant interfering ion background and varying cadmium concentration. Figure 7a shows the registered signals for samples with and without interfering ions. The selectivity coefficients were calculated from the cadmium concentration at the cross section of the two extrapolated linear segments of the calibration plot in analogy to ion-selective electrodes (Figure 7b) and by the background interfering ion concentration applying the following equation:  $\log K_{\text{Cd},\text{J}}^{\text{pot}} = \log([\text{Cd}^{2+}]/[\text{J}^{z+}]^{2/z})$ .

The formula with and without exponents was used as other authors reported<sup>20</sup> that, for ions of different charge, it did not give results representative of the observed experimental membrane performance using the exponents. The obtained detection limits were not significantly different from calibration curves in cadmium solutions without interference, except for lead and calcium ions (Figure 7b). The values would be more precise if calculated for higher interfering ion concentrations, but these quantities would not be realistic in environmental samples. Therefore, tabulated selectivity coefficients are approximated

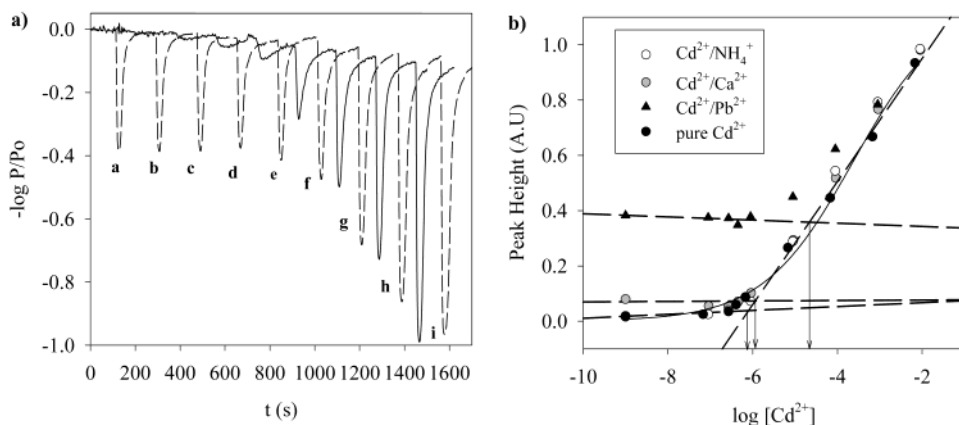


Figure 7. (a) Registered signals to evaluate lead interference. Solid line corresponds to the FIAGram obtained for different cadmium solutions; (a)  $10^{-9}$ , (b)  $6.8 \times 10^{-8}$ , (c)  $2 \times 10^{-7}$ , (d)  $3.4 \times 10^{-7}$ , (e)  $6.8 \times 10^{-7}$ , (f)  $6.8 \times 10^{-6}$ , (g)  $6.8 \times 10^{-5}$ , (h)  $6.8 \times 10^{-4}$ , and (i)  $6.8 \times 10^{-3}$  M. Dotted line corresponds to the same cadmium concentrations in a  $10^{-4}$  M lead solution. (b) Graphical method to evaluate the interference of the ions tested. Plotted calibration curves were obtained from samples containing a constant background of the interfering ions ( $10^{-3}$  M  $\text{Ca}(\text{NO}_3)_2$ ,  $10^{-3}$  M  $\text{NH}_4\text{NO}_3$ , or  $10^{-4}$  M  $\text{Pb}(\text{NO}_3)_2$ ).

Table 2. Selectivity Coefficient Values Obtained by the Fixed Interference Method Using the Expression with and without Exponent

interfering ions	selectivity coefficient $\log K_{\text{Cd},\text{I}}^{\text{pot}}$	
	with exponent	without exponent
$\text{Na}^+$	-0.15	-3.11
$\text{K}^+$	-0.29	-3.22
$\text{NH}_4^+$	-0.17	-3.17
$\text{Ca}^{2+}$	-2.93	-2.93
$\text{Zn}^{2+}$	-3.79	-3.79
$\text{Al}^{3+}$	-4.32	-3.32
$\text{Cu}^{2+}$		
$\text{Pb}^{2+}$	-0.76	-0.76

values that reflect the experimental results and prove the appropriateness of the tested new ketocyanine dye compared with the ones obtained using the same ionophore in other membrane compositions<sup>22</sup> (Table 2).

In general, the selectivity over alkali and alkaline-earth metals and transition metals was good with the exception of lead and copper ions. In the case of samples containing lead and cadmium ions, the membrane indistinctly detected both analytes; therefore, the employed ionophore (ETH 5435) can be considered selective for both ions in accordance with the previously reported papers for lead detection<sup>33, 34</sup> or more selective for cadmium as Simon and co-workers demonstrated.<sup>28</sup> Copper ion irreversibly interfered in the response, so its interaction was thoroughly studied spectrophotometrically. Spectra of the bulk optode in contact with a 0.1 M acetic/acetate buffer at pH 5.0, a  $10^{-6}$  and  $10^{-5}$  M  $\text{Cd}(\text{NO}_3)_2$  solution, and a  $10^{-6}$  M  $\text{Cu}(\text{NO}_3)_2$  solution were taken (Figure 8). The protonated form of ketocyanine 5ee presented a sharp peak at 771.6 nm when the membrane was in contact with the conditioning solution. When cadmium ions entered the membrane, the chromoionophore released protons to the solution to maintain electroneutrality. The absorbance of this peak, related to the acid form, decreased while the peak related to the basic form at 626.0 nm increased, showing a net isosbestic point at 682.1 nm. However, when copper ions entered the membrane, another peak at shorter wavelengths appeared (479.6 nm), demonstrating some

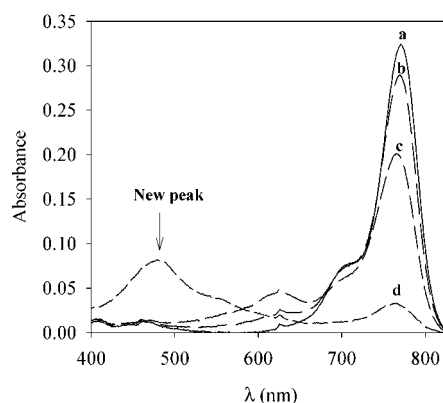


Figure 8. Recorded absorption spectra of the cadmium-selective optode in contact with cadmium and copper solutions. (a) 0.1 M acetic/acetate buffer at pH 5.0, (b)  $10^{-6}$  M  $\text{Cd}(\text{NO}_3)_2$  at pH 5.0, (c)  $10^{-5}$  M  $\text{Cd}(\text{NO}_3)_2$  at pH 5.0, and (d)  $10^{-6}$  M  $\text{Cu}(\text{NO}_3)_2$ . The chromoionophore is deprotonated with increasing  $\text{Cd}^{2+}$  concentration but irreversibly decomposes in the  $\text{Cu}^{2+}$  solution.

kind of interaction that irreversibly changed the dye resonance in the membrane and, thus, the absorption peak. With this membrane composition it is clearly noticeable that samples containing copper ions could not be monitored using the present sensor, but the assayed FIA system allows a sample pretreatment, so a complexing agent could be introduced in the carrier solution to remove copper before the optical detection.

**Short Time Repeatability and Lifetime.** The short time repeatability of the analytical signal was evaluated by successive repeated injections of the same solution (0.7 ppm cadmium). A relative standard deviation of 4.5% was obtained. As can be seen in Figure 9a, the signal is reversible enough to a reasonable time scale.

The performance of the sensitivity, calculated as the slope of the calibration curve, was followed over time to evaluate reproducibility (Figure 9b). The lifetime of the bulk optode depends on the number of calibrations performed as well as the exposure time of the sensor under light. The signal decreased 5% with 16 complete calibration experiments, and the calculated half-life time was  $t_{1/2} = 96.67$  h, so optimistic results could be expected for sensors stored in the dark.

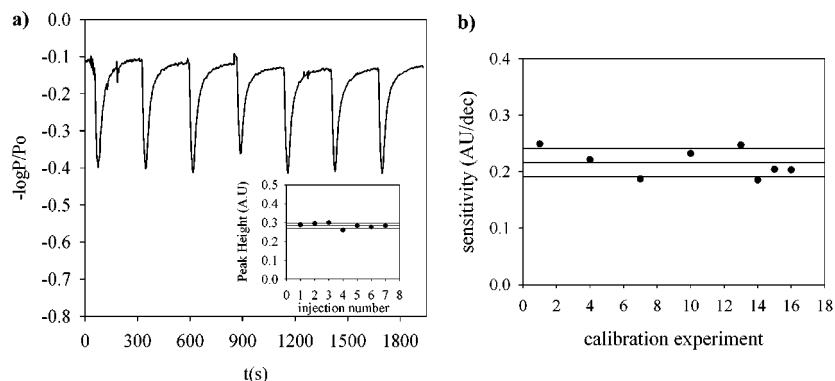


Figure 9. (a) Recorder output of the FIA system for 300- $\mu$ L successive injections of 0.7 ppm cadmium content at a sample rate of 2.1 mL/min. Replicated measurements are plotted with the mean value and the standard deviation. (b) Reproducibility as the variation of the slope of the calibration curve over the calibration experiments. Values are plotted with the mean and the standard deviation.

A decreasing trend of the baseline is expected for long time experiments because of the slowly photobleaching of the ketocyanine dye, which was reduced, attenuating laser power and preventing direct sunlight exposition of the membranes deposited over the transducer. However, membrane lifetime is not a limiting cause for the application of these optodes to real measurements, because making use of the improved IWAO, it is possible to easily renew the sensitive region when response characteristics are quenched. The disposable transducer can be changed to another or can be disconnected from the base holder and then reactivated, depositing another membrane. Although the employed deposition technique was less reproducible than other existing techniques such as the spin-on, the sensor-to-sensor reproducibility evaluated for four different deposited membranes as the peak height for the 1 ppm cadmium injection gave a peak height average of 0.24 AU, with a standard deviation of  $RSD = 7.5\%$ . Hence, freshly prepared optodes can be easily obtained for continuous monitoring, and reproducible techniques such as the spin-on technique can be used to ensure a more reproducible membrane thickness.

## CONCLUSIONS

A technologically improved IWAO prototype for ion detection was developed and evaluated in the present work. Such a device is presented as a versatile platform for the development of ion-

selective optical sensors, depending on the membrane composition, and permits to obtain disposable transducers.

Results demonstrated the suitability of this type of sensor to be employed as detectors in flow injection systems because of the short response times observed using the deposited thin membranes and without compromising sensitivity. Moreover, ketocyanine dyes have been proved applicable in combination with an ionophore giving highly sensitive responses. At this first stage of sensor development, satisfactory results for cadmium detection were obtained and promising alternatives are argued to improve the detection limit as well as the reproducibility. Actually, a sample pretreatment is under study to avoid the copper–chromoionophore interaction and other ketocyanine dyes of different basicities are being tested.

## ACKNOWLEDGMENT

The authors thank the Spanish CICYT agency (through project TIC97-0594-C04-02) for financial support of the present work.

Received for review January 14, 2002. Accepted May 1, 2002.

AC025520M